Journal of Contaminant Hydrology 222 (2019) 17–30

Contents lists available at ScienceDirect

Journal of Contaminant Hydrology

journal homepage: www.elsevier.com/locate/jconhyd

Flow field dynamics and high ethanol content in gasohol blends enhance BTEX migration and biodegradation in groundwater

Fabrizio Rama*, Débora Toledo Ramos, Juliana Braun Müller, Henry Xavier Corseuil, Konrad Miotliński

Núcleo Ressacada de Pesquisas Em Meio Ambiente (REMA) - Department of Sanitary and Environmental Engineering, Federal University of Santa Catarina (UFSC), Campus Universitário Sul da Ilha - Rua José Olímpio da Silva, 1326 - Bairro Tapera, 88049-500 Florianópolis, SC, Brazil

ARTICLE INFO

Keywords:
Transient flow
Dissolution
BTEX
Plume spreading
Biodegradation rate
Transport

ABSTRACT

Gasohol spills may easily descend through the soil column down and impact sensitive receptors as contaminants dissolve into the groundwater. Gasoline formulations are commonly blended with ethanol to alleviate environmental and economic issues associated with fossil fuels. However, the amount of ethanol added to gasoline and the groundwater hydraulic regime can significantly affect BTEX plume dynamics and lifespan. In this study, two long-term (5 and 10 years) field-scale gasohol releases with ethanol contents of 85% (E85) and 24% (E24), respectively, were assessed to discern the different dynamics undergone by gasohol blends. Statistical, geochemical, microbiological and trend approaches were employed to estimate the influence of groundwater flow variations on ethanol and dissolved BTEX transport, and the associated biodegradation rates of different gasohol blend spills. Ethanol and BTEX groundwater flow were quantified in terms of breakthrough curve characteristics, plume centroid positions and spreading, source depletion and mass degradation rates. In addition, bromide migration was evaluated to address the contribution of flow-driven dissolution. Results revealed that the high amount of ethanol along with a fast and dynamic flow exerted a flushing behavior that enhanced BTEX dissolution, migration (vertical and horizontal) and concentrations in groundwater. The higher amount of ethanol in E85 enhanced BTEX dissolution (and bioavailability) relative to E24 site and led to faster biodegradation rates, which can be explained by the cosolvency effect and metabolic flux dilution. Therefore, flow field dynamics and high ethanol content in gasohol blends enhance BTEX migration and biodegradation in gasohol-contaminated sites. The balance of these factors is crucial to determine fate and transport of contaminants in field sites. These findings suggest that hydraulic regime should be spatially and temporally characterized to support decisions on appropriate monitoring plan and remedial strategies for gasohol spills.

1. Introduction

Gasohol spills by accidental or incidental releases may readily descend through the soil column and pollute the subsurface. The dissolution of highly toxic and recalcitrant organic compounds present in gasoline can pose serious threats to human health and groundwater resources, as they are transported away from the source and can potentially reach sensitive receptors. Ethanol was primarily added to gasoline to replace MTBE (methyl tertiary-butyl ether) and reduce the environmental impacts related with MTBE high solubility and low biodegradation rates (Powers et al., 2001). Consequently, the incidence of ethanol-gasoline blends contamination increased as MTBE was phased out. The fate and transport of the organic compounds in the subsurface are generally affected by several processes such as volatilization, dissolution, advection, dispersion, diffusion, sorption and biological transformations (Schirmer and Butler, 2004). Moreover, the presence of ethanol and gasoline in fuel storage facilities or contaminated areas can also affect their degradation and mobility in groundwater and thus, must be addressed to predict the fate of multiple organic compounds in dynamic aquifers (Molson et al., 2002). High ethanol concentrations (above 10%) can exert a cosolvency effect on organic compounds present in gasoline formulations, including priority contaminants such as monoaromatic hydrocarbons (benzene, toluene, ethyl-benzene, xylenes, known as BTEX) and increase their dissolution into the aqueous phase (Powers et al., 2001; Corseuil et al., 2004). This can lead to a fast and complete dissolution of NAPLs (Non-Aqueous

* Corresponding author.
E-mail addresses: fabrizio.rama@posgrad.ufsc.br (F. Rama), debora.toledo@posgrad.ufsc.br (D.T. Ramos), juliana.b.muller@posgrad.ufsc.br (J.B. Müller), henry.corseuil@ufsc.br (H.X. Corseuil), konrad.miotlinski@ufsc.br (K. Miotliński).

https://doi.org/10.1016/j.jconhyd.2019.01.003
Received 13 October 2018; Received in revised form 21 December 2018; Accepted 9 January 2019
Available online 11 January 2019
0169-7722/

Phase Liquids) source, resulting in higher groundwater downgradient concentrations of recalcitrant and carcinogenic compounds (e.g. benzene) (Brooks et al., 2004) that thereby, increase the associated risk of exposure.

The effect of ethanol on gasoline spills in the subsurface has been extensively studied and the main observed features can be summarized as follows: (1) cosolvency of several gasoline components (e.g. BTEX) enhancing their solubility in aqueous-phase and remobilizing pre-existing NAPLs (McDowell et al., 2003; Falta, 1998; Jawitz et al., 2000); (2) collapse of capillary fringe, which influences the vertical migration velocity and the lateral distribution of the free-product zone (Henry and Smith, 2002; Yu et al., 2009); (3) preferential ethanol biodegradation followed by the depletion of favorable electron acceptors (e.g. O_2, NO_3^-, Fe^{3+}, etc.) and lower BTEX biodegradation rates (Corseuil et al., 1998; Mackay et al., 2006); (4) decreasing sorption-related retardation of hydrocarbons (Da Silva and Alvarez, 2002); (5) microbial biostimulation and growth inhibition at high ethanol concentrations ($10\ g{\cdot}L^{-1}$), (Cápiro et al., 2008; Rasa et al., 2013). In addition to this, some studies underlined a preferential retention of ethanol in vadose zone and into capillary fringe due to the partitioning to the pore-water (McDowell and Powers, 2003). Nevertheless, McDowell and Powers (2003) carried out their studies under stationary water table, whereas natural water table fluctuations cause capillary fringe mixing (Fetter, 2001) and may further release retained ethanol. These confounding effects may be mitigated under laboratory conditions (Gomez et al., 2008; Yu et al., 2009). However, laboratory studies are unable to reproduce a complex natural environment or account for field site-specific conditions and phenomena. To discern the effect of ethanol in gasohol blends on aromatic hydrocarbons biodegradation, Freitas et al. (2011) carried out field experiments of contaminant spills without ethanol (E0), as well as in gasohol mixtures with 10% (E10) and 95% (E95) of ethanol. The results demonstrated that BTEX biodegradation rates in groundwater were lower for high ethanol gasohol blends due to depletion of available dissolved oxygen, whilst for the no-ethanol spill and the low ethanol content blend no significant effect on BTEX biodegradation rates was observed. Conversely, Gomez and Alvarez (2010) used a numerical model to study the effects of five alcohols on the natural attenuation of benzene and claimed that high–ethanol content fuels (i.e. E85) result in smaller, shorter-lived benzene plumes in groundwater when compared to low–ethanol blends (i.e. E10). Corseuil et al. (2011a) observed a short-lived inhibitory effect of ethanol and acetate on BTEX biodegradation, demonstrating that monitored natural attenuation (MNA) can be a viable remediation strategy to deal with gasohol residual sources (E24). Corseuil et al. (2015) demonstrated the potential benefits of augmenting the electron acceptor pool with nitrate to accelerate ethanol removal mitigate its inhibitory effects on BTEX compounds and speed up their biodegradation. Lastly, Steiner et al. (2018) showed that for gasohol blends with low-ethanol content (i.e., 10%), MNA can provide slightly higher BTEX degradation rates compared to nitrate biostimulation, provided that the aquifer geochemical conditions offer a sufficient electron acceptor pool for aromatic hydrocarbons biodegradation.

Field studies normally conduct limited spatial and temporal hydrogeological characterization of groundwater that can be conducive to unreliable monitoring plans and negatively affect remediation strategies. Shallow aquifers, which are commonly affected by contamination, often exhibit a significant temporal variability in water level position, thickness of unsaturated and capillary zones and directions of groundwater flow which may affect migration, dissolution and biodegradation rates (Davis et al., 1999; Prommer et al., 2002; Zhang et al., 2009). Rein et al. (2009) showed through numerical simulations that transient flow conditions represent a critical source of uncertainties in field measurements, as they are conducive to significant temporal fluctuations of the contaminants concentration in the monitoring wells. Dobson et al. (2007) demonstrated that water-table fluctuations in contaminated aquifers increased the elution of dissolved LNAPL components and thus, enhanced the risk of exposure of downgradient receptors. In addition, water-table fluctuations along with transient changes in groundwater direction and flow focusing into highly permeable heterogeneities are claimed to be the main drivers for solute mixing, especially for transverse plume spreading (Werth et al., 2006; Rolle et al., 2009). Since biodegradation rates may be controlled by the mixing process, which supports interchanges between electron donor and acceptor (Cirpka et al., 1999), recharge events may result in higher biodegradation rates by means of groundwater fluctuations and oxygen mixing (Schirmer et al., 2000). Although limited attention has been given towards transient hydraulic effects in full-scale experiments, they can have an overriding significance for monitoring plans and remediation strategies for gasohol spills.

In this contribution, two long-term (5 and 10 years) controlled releases of gasohol blends (E85 and E24) were monitored to discern the role exerted by groundwater flow dynamics on ethanol/BTEX plumes migration and degradation rates. This work aims to advance the current understanding on gasohol spills with different ethanol content and overall site remediation by addressing the contribution of groundwater flow field and site-specific transport rates on ethanol and BTEX plume dynamics and lifespan.

2. Materials and methods

2.1. Site description

The controlled releases of gasohol blends were carried out at Ressacada Experimental Farm, in Florianopolis, Santa Catarina, Brazil (latitude 27°30′S, longitude 48°30′W) (Fig. 1). The climate is humid subtropical with average groundwater temperature of 22 °C and mean annual precipitation varies from 1100 to 2700 $mm{\cdot}y^{-1}$. Rainfall is highly variable and more intense during the summer season. The study area represents a shallow coastal aquifer (30–40 m thick) with an average depth to water level in the range of 0.3 to 2.0 m, featured by sharp and quick transient fluctuations driven by rainfall events (Rama et al., 2017). The aquifer is located in a flat coastal plain (up to 5 m in elevation) of about 20 km^2, enclosed by surface water bodies. Nevertheless, the tidal fluctuations have negligible influence on water-table levels when compared to rainfall infiltration (Rama et al., 2018). A dense net of rivers, ponds and anthropogenic ditches controls groundwater drainage in the plain (Fig. 1).

The aquifer is composed of unconsolidated deposits of lacustrine and marine fine quartz sands with hydraulic conductivity values in the range of 10^{-3} to $10^{-4}\ cm.s^{-1}$ (Lage, 2005). Irregularly distributed lenses of silt and clay are present in the plain and mangrove swamps areas are located at surface water receptors. The typical subsurface sample contains about 90% of sand, 3% of silt and 7% of clay, although higher silt and clay contents (up to 20%) were observed in several samples (Lage, 2005). The average organic matter content in the top layer (0.82 m depth) is 1.16% and decreases in a vertical direction (from 2 to 4 m depth) to 0.06% (standard deviation of 0.03%) (Fernandes, 2002).

2.2. E85 field experiment

The experiment was established by releasing 200 L of E85 (85% ethanol and 15% gasoline v/v) and 2.5 kg of the conservative tracer - potassium bromide (previously diluted in the 200 L-blend) into an excavated pit of 1.5 × 1.0 × 0.25 m in the unsaturated zone (Fig. 2). When the experiment started (September 8, 2010), the water-table depth was 1.6 m below ground surface (bgs) or 1.35 m below the bottom of the excavation pit. The area was monitored with a total of 50 multilevel (2, 3, 4, 5 and 6 m bgs) monitoring wells (MW). Groundwater sampling was conducted using a peristaltic pump connected to each level by a polyethylene tubing (Fig. 2b). The wells were installed downgradient to the source of contamination (NW-SE). The free-

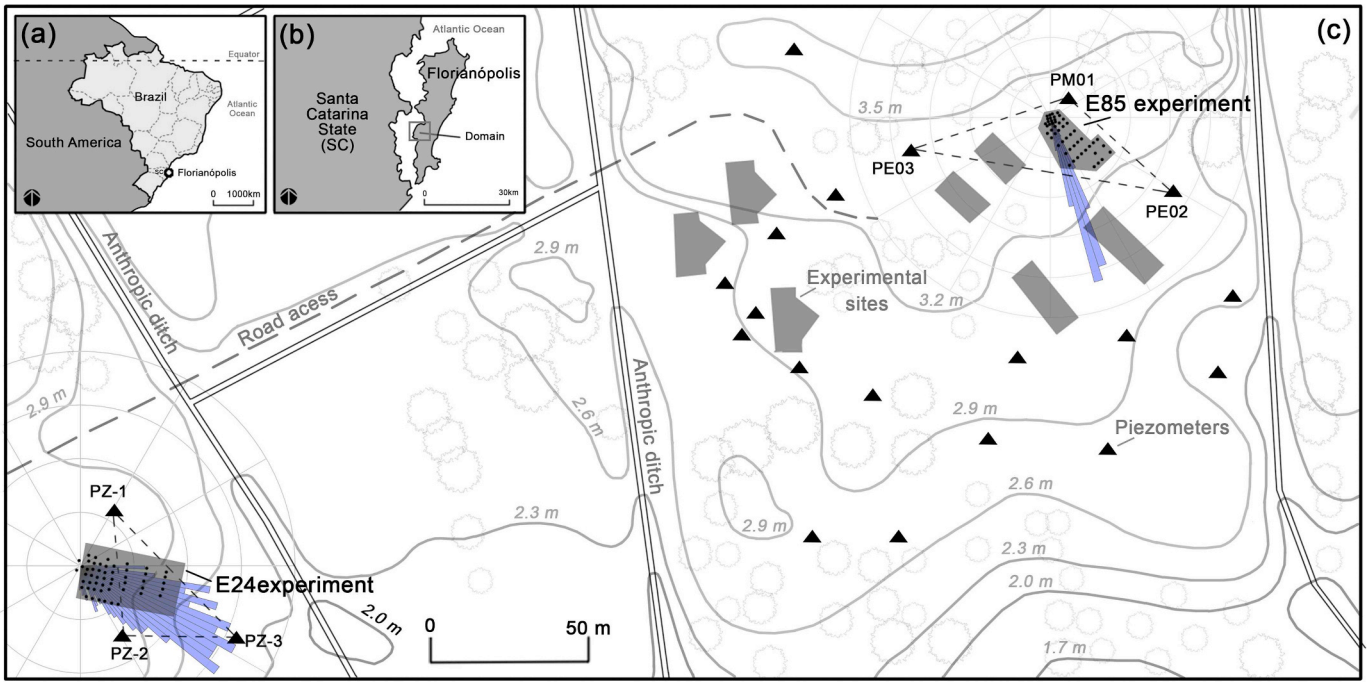

Fig. 1. Location of experimental sites: (a) map of Brazil; (b) map of Florianopolis; (c) detailed map of the E24 and E85 experimental sites depicting the monitoring wells (black points), local directions of groundwater flow estimated according to the method described in Section 2.5 (light blue polar diagram), piezometers positions (black triangles) and designations (e.g. PE03, PZ-1, etc.), surface elevation above mean sea level (light grey isolines and numbers in italic) and other field experiments (grey polygons). (For interpretation of the references to colour in this figure legend, the reader is referred to the web version of this article.)

product zone (FPZ), which represents the free NAPL "floated" on the top of the aquifer as a result of infiltration process, extends beyond the source zone affecting a larger area (bright red area in Fig. 2c). A recharge ratio of 43% of precipitation varies from 36 to 52% on a monthly basis (Rama et al., 2018). Groundwater background geochemical conditions were: pH 4.9 +/− 0.2; specific conductance 0.04 +/− 0.008 µS/cm; redox potential 191 +/− 60 mV, bromide 0.05 +/− 0.03 mg L^{-1} and phosphate 0.09 +/− 0.03 mg L^{-1}. Background electron acceptors concentrations and shifts over time are available in the Supporting Information (Table S1).

An adjacent field experiment with E24 (24% ethanol and 76% gasoline v/v) located at a distance of 400 m (Fig. 1c) was used to provide insight into the different dynamics undergone by gasohol blends with a different ethanol content (85% and 24%), source position relative to the water table (135 and 0 cm, for E85 and E24 respectively) and local flow field conditions. This experiment started in 1998 with the release of 100 L of E24 blend into a 1.5 × 1.0 × 1.5 m pit (Corseuil et al., 2011a). Both experimental sites were covered with a plastic impermeable canvas overlaid by coarse uniform gravel to avoid direct rainfall infiltration.

The mean hydraulic conductivity values estimated with slug tests were 8.81×10^{-4} cm.s^{-1} and 1.1×10^{-4} cm.s^{-1} (Corseuil et al., 2011b) at E85 and E24, respectively. The average hydraulic gradient at E24 (0.011 +/− 0.0041 m/m) was approximately two times higher than at E85 (0.0067 +/− 0.0018 m/m). Saturated effective porosity was 0.2 (Corseuil et al., 2011b) and 0.28 (Müller et al., 2017) at E24 and E85, respectively. These data were used to calculate the local seepage velocities by applying the Darcy's law.

2.3. Physical and geochemical analysis

The E85 biodegradation and migration were monitored through ethanol and BTEX concentrations and their anaerobic metabolites, acetate and methane. Background groundwater geochemical conditions were determined at sampling events conducted at 160 and 41 days before the release. After E85 was released, 15 sampling events (SE) were conducted over 1540 days: the first 10 SE (sampling interval 1 to 15 days) aimed to monitor source depletion and mass-transfer mechanisms, while SE 11 to 15 (sampling interval 6–12 months) focused on plumes migration. Oxidation-reduction potential (ORP), pH and dissolved oxygen were measured on site using a Micropurge Flow Cell (MP20) and a peristaltic pump (Millipore Easy-Load model XX80EL000). Bromide and acetate were analyzed by ion chromatography using a Dionex ICS-3000 equipped with a conductivity detector (Software Chromeleon PN 6.40), an AS4A-SC column, with two eluents: sodium carbonate and sodium bicarbonate (APHA, 1992). BTEX, ethanol and methane were measured by gas chromatography with a HP 6890 II chromatographer coupled with a HP 7694 headspace auto sampler and a flame ionization detector (FID). A methyl-siloxane capillary column, HP 1 (30 m × 0.53 mm × 2.65 µm) was used. Samples were collected into capped sterile glass vials without headspace to prevent volatilization losses. Detection limits were as follows: bromide (0.1 mg.L^{-1}), acetate (1 mg.L^{-1}), ethanol (1 mg.L^{-1}), methane (10 µg.L^{-1}) and BTEX (1 µg.L^{-1}). Free-phase NAPL samples or free-product samples (FPS) indicate water samples that show visible dual-phase or a BTEX concentration above aqueous saturation limits, and for this reason were not accounted in the dissolved mass.

Transient hydraulic gradients and directions were estimated from the triangulation of the closest hydraulic head records in both experiments to allow a reliable flow field reconstruction over time (Fig. 2a). Water level was monitored by a manual phreatimeter with variable recording intervals (1–60 days). Saturated hydraulic conductivity was estimated from two slug test campaigns in different seasons (summer and autumn). Bouwer and Rice method was utilized to interpret the data and to determine hydraulic conductivity (Butler Jr., 1997).

2.4. Microbial analysis

Real-time quantitative polymerase chain reaction (qPCR) was used to estimate the concentration of total Bacteria to evaluate bacterial growth and Archaea (groups Crenarchaeota and Euryarchaeota), which includes methanogens. A total of 5 sampling events before

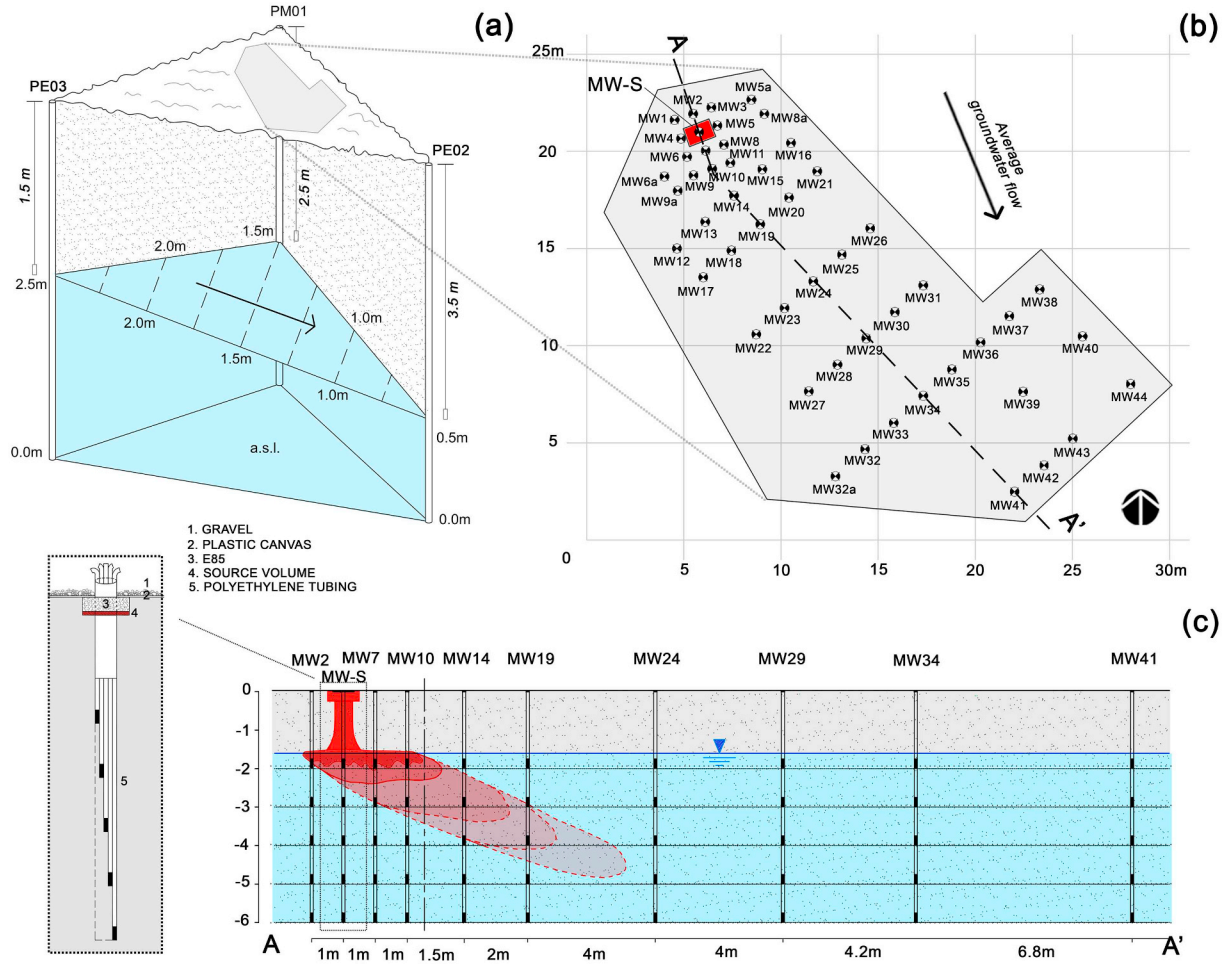

Fig. 2. E85 experiment conceptual sketch: (a) geometrical interpretation of water-table inclination and groundwater flow direction; (b) position of 50 multilevel monitoring wells (circles), source area (red rectangle) and the mask adopted for the plume interpolation (grey area); (c) A-A' transect with conceptual gasohol distribution and detailed sketch of monitoring well with sampling depths configurations. (For interpretation of the references to colour in this figure legend, the reader is referred to the web version of this article.)

(background) and after the release (72; 918; 1161 and 1532 days after the release) were conducted at the E85 site. For DNA extraction, 1 L of groundwater was collected and samples were subsequently filtered with a 0.22 mm Millipore membrane filter (Sartorius Stedim Biotech, Gottingen, Germany). DNA was extracted using a MoBio Power Soil™ (Carlsbad, CA) kit, following the manufacturer's protocol. Primer sequences and PCR assays details can be found elsewhere (Ramos et al., 2013). Next-generation sequencing (16S rRNA gene sequencing) were conducted for E85 experiment (MW-23 at 1161 days after the release and MW-25 and source at 1532 days) to characterize microbial populations profile at the site. Briefly, Illumina Miseq platform was used for the sequencing of regions V3 and V4 that were amplified by PCR. Bioinformatics was conducted by the Quantitative Insights Into Microbial Ecology (QUIIME, v1.9.0, http://qiime.org/index.html) software and Greengenes was used as database to obtain taxonomic information. Details are described in Müller et al. (2017).

2.5. Hydrogeological and statistical data processing

Different lines of evidences (LoE) were used to discern the ongoing predominant biotic and abiotic processes in the experimental sites. Accordingly, in order to associate plume migration, maximum concentration occurrences and flow field variations, geometrical rules were applied to triangulate information from monitored head records, simplifying the unconfined aquifer with a plane. As depicted in Fig. 2a, the plane was defined by passing through three points to establish the dip angle and direction (strike +90°), which represent the water-table inclination and the direction of groundwater flow, respectively. In addition, geochemical and microbial analyses were employed to evaluate the different dynamics undergone by E85 and E24 blends in groundwater. An exploratory analysis on concentrations was conducted for the conservative tracer (bromide), organic contaminants (ethanol and BTEX) and main metabolites (methane and acetate). The dataset was previously transformed to deal with the large amount of data assigned as below the detection limit (BDL) or non-detected values (ND).

Means and standard deviations for each series were calculated from a linear regression of expected normal scores (*Z*-scores) (Gineval and Splitstone, 2003). The methodology consists in a linear regression of the known standard concentrations, firstly converting the ranks of the data into cumulative percentiles. Observations from a normal distribution tend to fall on a straight line when plotted against their Z-Scores, even for ND values. Thus, the fitting line intercept indicate the mean of distribution, while the slope of the line gives the standard deviation. Such values were used to fix NDs data following the same distribution of the raw data (Fig. S1 - Supporting Information). Hence, a normal distribution was applied to NDs in the dataset.

The cosolvency model was applied to distinguish the BTEX free-product from the dissolved-phase in full-scale experiments with high-ethanol blends (Corseuil and Fernandes, 1999; Powers et al., 2001). The model states that ethanol (a hydrophilic compound) can reduce the

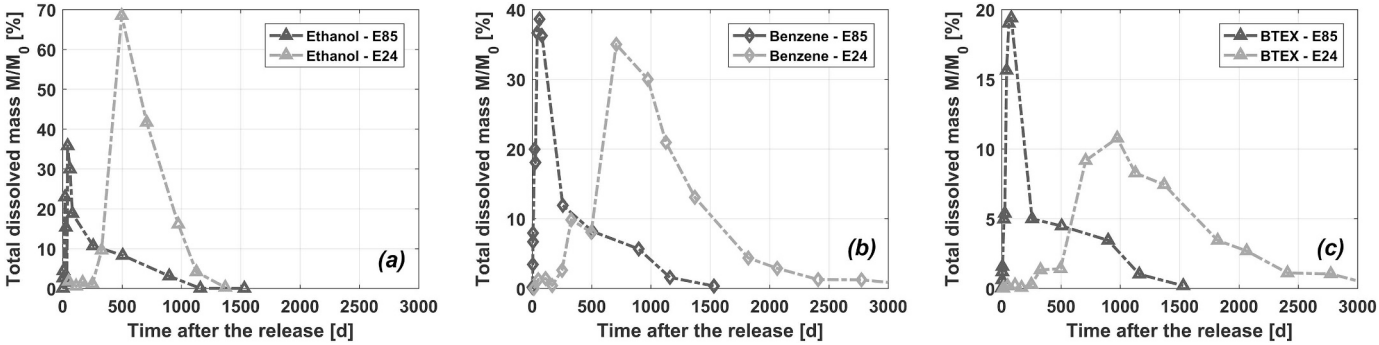

Fig. 3. Total dissolved mass (%) over time: (a) ethanol, (b) benzene, and (c) BTEX in E85 and E24 experimental sites.

polarity of aqueous phase, modifying the solubility of hydrocarbons in groundwater systems and enhancing the saturation concentration based on Raoult's law. Detailed information about the calculus of the saturation concentration of BTEX at E85 site is available in the Supporting Information (Table S2).

The dissolution and persistence of ethanol and BTEX in groundwater, as well as the production of their corresponding metabolites (acetate and methane) were graphically depicted on the breakthrough curves of concentration (BTC). Plume stability and trend analysis for bromide, ethanol and BTEX were built using MATLAB to assess sites under natural attenuation with a well-established and consistent monitoring over a given time frame (Ricker, 2008). The method is applied only to dissolved contaminants and corresponds to a combination of graphical and statistical analysis, based on the spatial interpolation of data from multilevel monitoring wells in the experimental site, aiming to define isocontour maps for every compound, depth levels and SE. This allows the calculation of dissolved mass in every SE by summing results per level. Detection limits (DL) were used to contour plumes for each compound. While a 35 × 30 × 5.5 m domain was applied for E24 area, a 33 × 33 × 7 m domain was used for the interpolation of E85 data, both deploying a regular grid spacing of 0.1 × 0.1 × 0.25 m. A mask was adopted to limit extrapolated values out of the monitored sites (Fig. 2b). Raw concentration data were log transformed to obtain normal distribution and reduced coefficient of variation (ratio of standard deviation and mean) and kriging interpolator was used to plot contour maps.

The zero-order momentum of concentration over time was used to estimate total dissolved mass at the site. Plume centroid position was obtained by the estimation of first-order momentum. A plume center of mass represents the centroid of interpolated contour plume. Conceptually, it is a mass weighed-mean of every unit volume along three main directions (Freyberg, 1986; Dentz et al., 2000). The position of mass centroid was chosen to represent plume migration less sensitive to heterogeneous spatial distribution of contaminants. Finally, neglecting the local-scale mixing, the estimation of central second-order spatial moments provided direct plume-spreading information (Cirpka, 2002). Therefore, in order to quantify combined impacts of groundwater flow and the ethanol cosolvency in both areas, plumes lifespan (normalized dissolved mass, centroid position, distance to source, spreading) were plotted over time. Total accuracy of the method was equal to maximum mass recovery of dissolved bromide (about 66% of initial released mass). The mass losses can be related to experimental limitations, such as spacing between monitoring wells and depth levels, gaps between sampling events or spatial interpolation efficiency.

The linear fitting (zero-order kinetics) of bromide mass decrease was used to represent migration of compounds (forced by groundwater flow field) beyond the assumed mask. Site-specific transport rates were estimated by dividing bromide zero-order fitting rates for the total bromide mass released. First-order kinetics are commonly used to describe BTEX and ethanol degradation rates in aquifers, by fitting dissolved masses versus time to an exponential decay model (Alvarez and Illman, 2006; Corseuil et al., 2015; Steiner et al., 2018). Nonetheless, these rates do not discern between migration and biodegradation processes. Thus, biodegradation rates were obtained by subtracting transport rates (bromide advective-dispersive transport-related) from the reactive compounds first-order degradation rates. Finally, ethanol and BTEX biodegradation rates were determined after the onset of ethanol and BTEX degradation.

3. Results and discussion

3.1. Centroid analysis, plume migration and groundwater flow field

The ethanol content in different gasohol blends can markedly affect aromatic hydrocarbons dissolution into the groundwater. Accordingly, in E85 plot BTEX compounds exhibited a faster and enhanced dissolution relative to E24 (Fig. 3). This was attributed to the cosolvency effect exerted by high dissolved mass of ethanol (≈ 50 kg) that thereby enhanced aromatic hydrocarbons dissolution and resulted in high BTEX plume concentrations (≈ 20 mg L^{-1}). The fast ethanol and BTEX dissolution into the groundwater was evidenced by the peak of dissolved mass after 42 and 83 days, respectively (Fig. 3a and Fig. 3c). This implies that high concentrations of dissolved BTEX can rapidly migrate away from the source zone, enhancing the potential risk to downgradient sensitive receptors. In contrast, BTEX compounds dissolution and corresponding aqueous average concentrations were significantly lower in E24 site (≈ 5 mg L^{-1}), as ethanol content was probably not high enough (less than 15 kg) to exert cosolvency effect. The E24 site showed a typically slow dissolution of aromatic hydrocarbons (Corseuil et al., 2011a), reaching a maximum dissolved mass at 1000 days following the release, which corresponded to the half of the observed percentage for BTEX in E85 plot (Fig. 3c). Thus, although the amount of gasoline released in E24 (76 L) was 2.5 times higher than in E85 (30 L), BTEX compounds exhibited an opposite trend by rapidly (after 83 days) reaching peak dissolved concentrations and dissolved mass percentage in E85 site, due to the cosolvency effect exerted by the high ethanol content in the gasohol blend.

The cosolvency effect was more apparent for the higher molecular weight and less soluble BTEX compounds (ethyl-benzene and xylenes), while benzene presented similar maximum dissolved percentage in both E24 and E85 sites (Fig. 3b). Thus, BTEX plot showed that 12% of initial mass was dissolved in E24 while such percentage increased to about 20% in E85 (Fig. 3c). This behavior is justified by the ratio of the saturation concentration (enhanced by the cosolvency) to the original compound solubility (Table S2 - Supporting Information). Such ratio, which increased with the molecular weight, indicates the effect of the cosolvency on enhancing the maximum solubility of the compound and results in significantly higher dissolved mass for ethyl-benzene (3.7) and xylenes (3.8) relative to benzene (1.9). Hence, the difference in the maximum dissolved mass between E24 and E85 was more pronounced

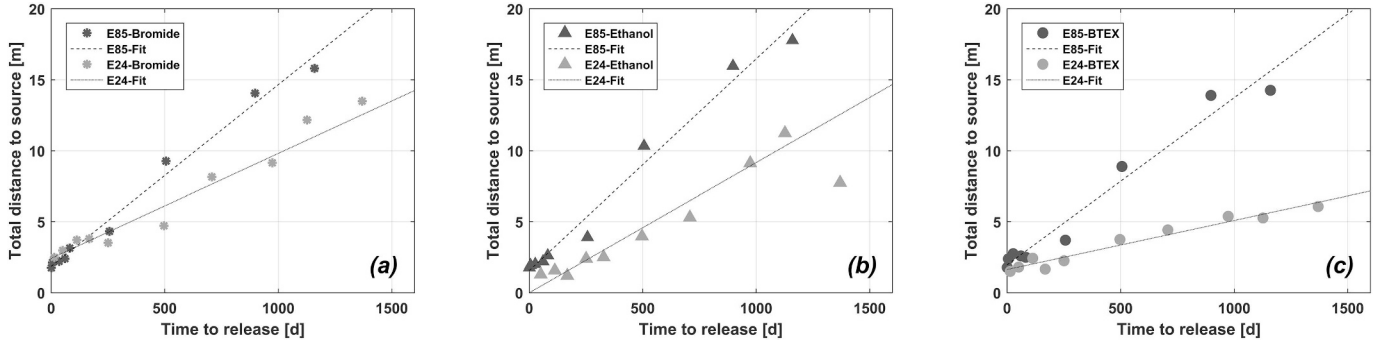

Fig. 4. Plume centroid migration: (a) bromide, (b) ethanol, and (c) BTEX in E24 and E85 sites. Dotted fitting lines represent plume centroid velocity.

for ethyl-benzene and xylenes than benzene.

Contaminant plumes are typically formed after compounds dissolve into the groundwater and their behavior (e.g. position, geometry) is highly dependent on the hydraulic regime (Dobson et al., 2007). Accordingly, at E85 the BTEX, ethanol and bromide plumes migrated concomitantly, at similar velocities (between 4.5 and 6.2 $m \cdot y^{-1}$) and followed the local groundwater flow direction, moving faster in horizontal and downward directions, as evidenced by the close position of centroids (Fig. 4 and Fig. 5). Conversely, at E24 the bromide, ethanol and BTEX plumes followed different migration pathways (Fig. 5). The ethanol plume velocity was similar (3.0 $m \cdot y^{-1}$) to bromide (2.6 $m \cdot y^{-1}$) but significantly higher than BTEX (1.2 $m \cdot y^{-1}$), which is probably due to a sorption-related retardation of hydrocarbons (Fig. 4). Therefore, at E24 the BTEX plume exhibited a limited migration of plume centroid (5 m away from the source) when compared to E85 (15 m) during the same timespan (Fig. 4c). The different dynamics undergone by BTEX, ethanol and bromide plumes in E85 and E24 sites was consistent with the average seepage velocities (Table 1). In addition, a direct correlation between water-table levels and seepage velocity was observed for both experimental sites (Fig. S2 and Fig. S3 - Supporting Information), which was attributed to the periodic increase of hydraulic gradients due to the intense and prolonged rainfall events (Rama et al., 2018). This led to transient accelerations in the transport of contaminants, as the gradients are directly proportional to the seepage velocity. Thus, ethanol apparently exerted influence on BTEX compounds dissolution in the source zone that was conducive to high groundwater concentrations, while plume dynamics were predominantly affected by hydraulic effects and groundwater flow.

The larger variability in groundwater direction and hydraulic gradient enhanced transversal spreading of plumes. Accordingly, despite the lower seepage velocity at E24, the bromide plume showed an enhanced dispersion relative to E85 (Fig. 5a) which is reflected by more dynamic groundwater flow (Table 1). These findings agreed with Bellin et al. (1996), who showed a plume dispersion affected by instability of

Table 1
Groundwater flow characteristics from the transient analysis.

	E85	E24
Precipitation [mm/y]: Range	1600–2200	
Recharge [%]: Mean (range)	43% (39–55%)	
Hydraulic conductivity [cm/s]	8.81×10^{-4}	1.1×10^{-4}
Saturated effective porosity [−]	0.28	0.2
Average water-table level [m]: Range	1.0–2.9	1.3–3.1
Gradient [m/m]: Mean (std. dev.)	0.0067 (0.0018)	0.0114 (0.0041)
Direction [degrees]: Mean (std. dev.)	161.2° (10°)	127.7° (30°)
Seepage velocity [m/y]: Mean (std. dev.)	6.7 (0.8)	2.0 (1.0)

the hydraulic gradient over time. Likewise, the total range of directions in E24 reached 90°, whereas in the E85 site it was limited to 30° (Fig. 1c). The E85 site was characterized by a slower shift of flow direction, with long periods (2–6 months) in which groundwater flow presented homogeneous deviations from the average direction. Low water levels were highly correlated with negative deviations of groundwater direction, as opposed to the higher levels that were associated with positive deviations (Fig. S2 - Supporting Information), suggesting an existence of a low-conductivity layer in the aquifer, which is probably dipped towards the east. Comparatively, in the E24 experiment, a more pronounced and quicker variability in the flow direction was observed (Fig. S3 - Supporting Information). The data suggests a random rotation of groundwater direction during intense rainfall events (with no evident correlation with hydraulic heads), which was likely attributed to the position of the finer and, consequently, less conductive material in the E24 site.

Heterogeneities in permeability along with impulsive precipitation and differences in land use led to a different infiltration regime and thus, a local variability in transient groundwater flow directions and recharge. It is worth highlighting that as little as 10–15% of fine material admixture in a soil profile is enough to confer a low-permeability character of the porous medium (Mitchell, 1976). Thus, despite its

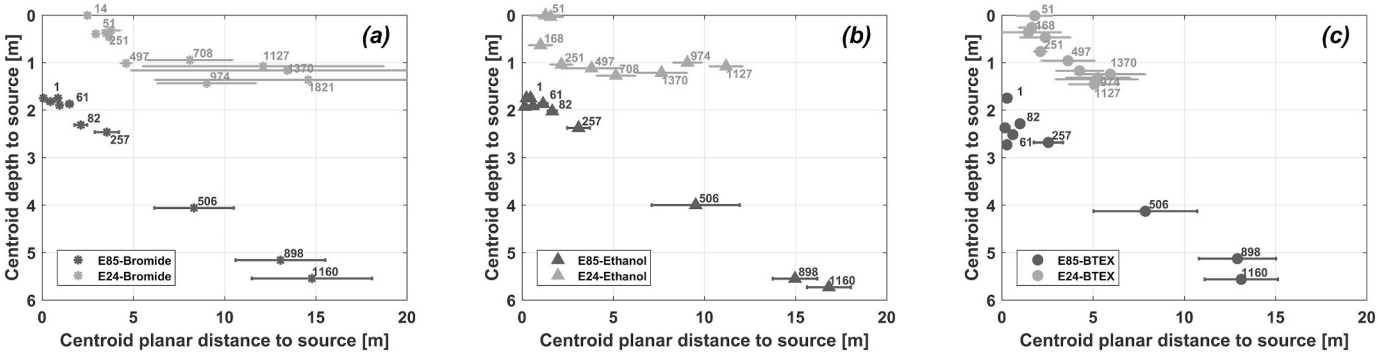

Fig. 5. Plume centroid position and spreading of (a) bromide, (b) ethanol, and (c) BTEX in E24 and E85 sites. Symbols represent centroid vertical and horizontal location (m) relative to source, bars show planar plume spreading (m) over time and numbers above the bars represent the time (days) after the release.

geological homogeneity at regional-scale, the existing clay content in the site (up to 20%) is sufficient to significantly influence the local flow field and the migration of compounds. In addition, the close relation between small low-permeability lenses and, hydrodynamic dispersion (Werth et al., 2006) or back diffusion of contaminants (Chapman and Parker, 2005; Yang et al., 2014) has been shown. This is also consistent with the enhanced plume spreading in the E24 relative to E85 site (Fig. 5).

The sharp water-table fluctuations may prevent the retention of dissolved compounds within and above the capillary fringe. The E85 mass center moved vertically very quickly when compared with the E24 site (Fig. 5). For example, at the E85 site between 257 and 506 days from release, the ethanol centroid moved more than 1.5 m downwards and 7 m in a horizontal direction away from the source, while BTEX plume migrated 1 m vertically and about 5 m horizontally. Such high velocities of contaminants vertical transport is likely due to the sudden water-table oscillations (recharge-related) that literally drag solutes downward, similar to a natural "vertical flushing" of the source zone. Conversely, in E24 site, the consistently lower conductivity of E24 (relative to E85) limited compounds transport, as evidenced by the low bromide ($^{>}$ 1.5 m downwards over 1821 days) and ethanol ($^{>}$ 1 m downwards over whole monitoring period) centroid vertical migration (Fig. 5). Nevertheless, since the amplitude of water-table fluctuations was similar in both sites (Fig. S2 and Fig. S3 - Supporting Information), the aquifer in E24 probably discharged laterally the flow related to the high hydraulic heads, as is the case for wetlands (Hayashi et al., 2016). Thus, the high variability of groundwater direction at the E24 may be caused by a hanged up "fill and spill" system (Tromp-Van Meerveld and McDonnell, 2006) with an irregular groundwater connectivity. It is worth noting that the influence of vertical infiltration from precipitation events was dismissed, as both sites were covered with plastic impermeable canvas and gravel. Therefore, the plumes behavior is attributed to the combined effects of natural Darcy's flow with "bottom-up" variations in water-table levels. The field data show that the transient flow regime directly affected spreading and position of the contaminants plumes (Davis et al., 1999). The flow field assessment indicated that the water-table plane in both experiments rotates in time, depending on the condition of recharge, heterogeneities and soil saturation. The faster and more regular groundwater flow in the E85 site seemed to be mainly related to the precipitation regime, while the highly variable flow field in the E24 site was probably forced to a lateral movement by hanged clay lenses and geological heterogeneities.

3.2. Geochemical footprint of E85 release

The statistical analysis depicted a lognormal distribution of ethanol and bromide concentrations at each sampling event for E85 plot (Fig. 6). Violin plots median values showed the faster dissolution of ethanol that peaked only 5 days after the release, while bromide maximum dissolution occurred 83 days after the release. Since bromide and the gasohol blend were released together, such differences reflect the higher aqueous solubility of ethanol relative to bromide. In addition, violin plots revealed a smoother variation of bromide shapes over time relative to the highly irregular ethanol distribution. This can be attributed to the conservative behavior of bromide as opposed to the highly biodegradable ethanol.

A highly variable water table may enhance BTEX dissolution from the source or the free-product zone (FPZ), and the subsequent outcome would be a vertical downward migration of contaminants as the water table descends. In gasohol spills, the dissolved ethanol, which "floats" on the top of an aquifer, can remobilize retained BTEX in the vadose zone (McDowell et al., 2003; Falta, 1998). This seems to be the case of the E85 source area, as the high dissolved concentrations of BTEX coincided with the increase in water level and the intense recharge events (Fig. 7). The contaminants (ethanol and BTEX) rapidly reached the water table moving vertically 1.3 m in one day (Fig. 5). Such fast migration was attributed to the root channels and other preferential transport pathways (Jarvis, 2007), which along with the high solubility of ethanol facilitates the movement. The high amount of ethanol could have also reduced the sorption of hydrocarbons, contributing to the vertical transfer of BTEX as well (Da Silva and Alvarez, 2002). During the initial water level increase (between 5 and 6 days after the release), the average concentration of BTEX in the aqueous-phase increased about 10 times, whereas after 20 days, a pronounced rising of aquifer

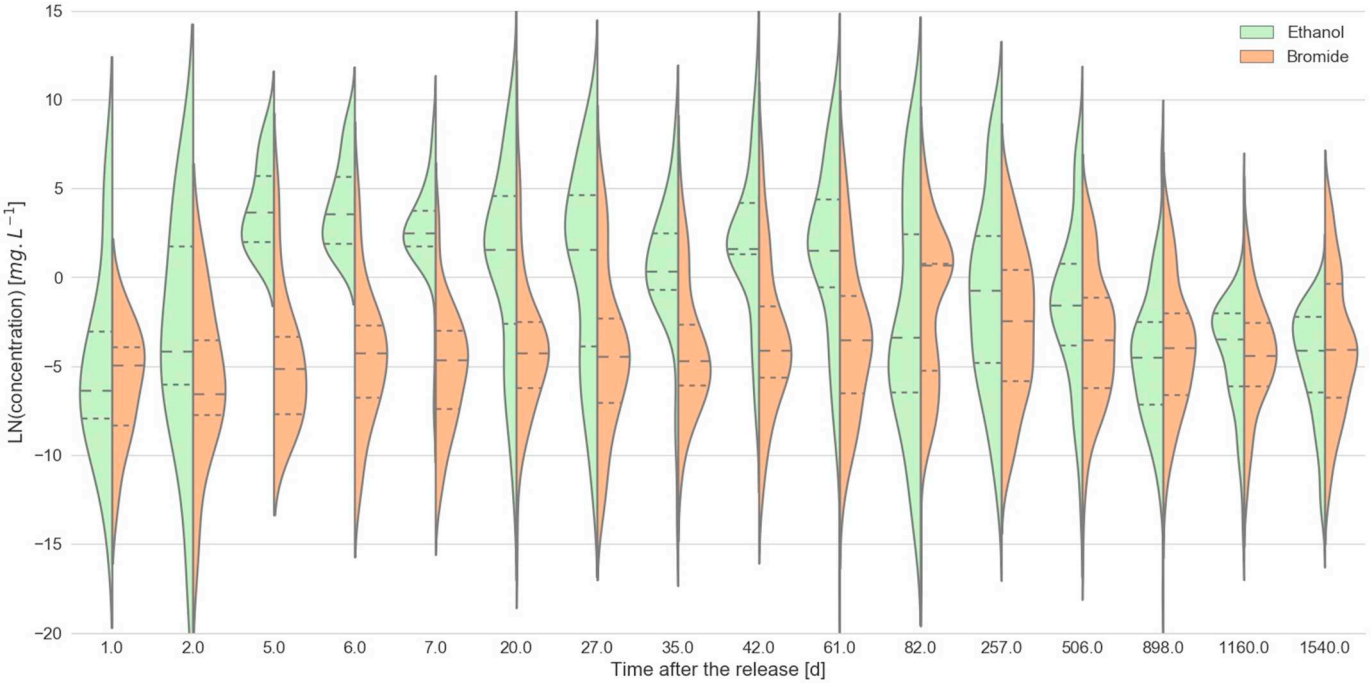

Fig. 6. Violin plot with distribution of bromide (salmon) and ethanol (green) concentrations. Loosely dashed lines represent the median, densely dashed lines are the interquartile intervals, while the shape of violins depicts the distribution. (For interpretation of the references to colour in this figure legend, the reader is referred to the web version of this article.)

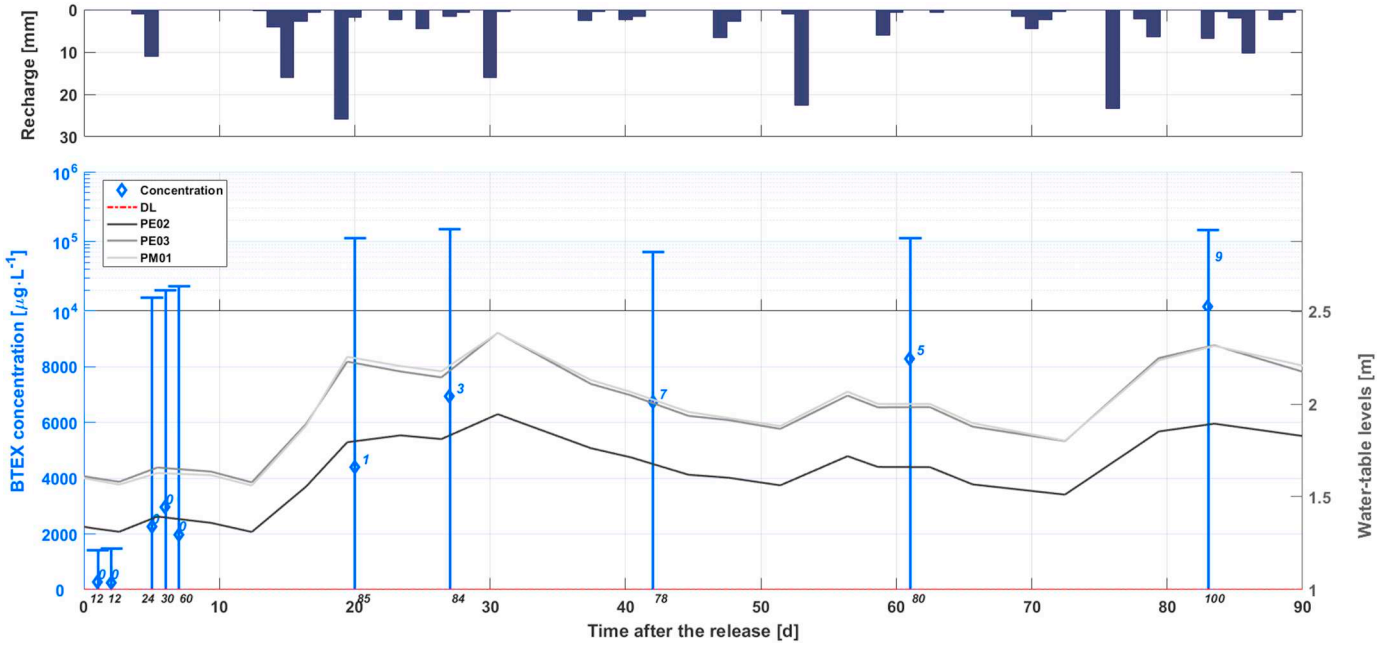

Fig. 7. Time series of average dissolved BTEX, water-table levels (dark and grey lines) and daily accumulated recharge (blue columns) within the first 90 days in the E85 site. The blue diamond markers represent mean values of concentration; errorbars show the range of concentrations; blue numbers represent the total of BTEX free-phase samples (FPS) in each sampling event, dashed red lines represent the detection limit and black numbers correspond to the total samples collected. (For interpretation of the references to colour in this figure legend, the reader is referred to the web version of this article.)

water table resulted in a pulse enhanced concentration up to three-fold. Lastly, between 42 and 83 days after the release, average concentrations of BTEX doubled and maximum values per sampling event continued to increase because of the high hydraulic head of the aquifer (Fig. 7). Thus, data confirmed a correlation between rainfall-driven processes (e.g. recharge, water-table variation) and the increasing dissolved BTEX concentrations in the source zone (Table S3 - Supporting Information).

The combined effects of ethanol and aquifer fluctuation must be carefully accounted in sites impacted by gasohol spills as they can accelerate dissolution process and may compromise remediation plans based on the slow transfer hypotheses of persistent LNAPL sources that generally results in long-lasting contaminations. Free-phase product sample (FPS) occurrences started 18 days after the release, when the water table reached 2.25 m above sea level (0.7 m depth underneath the source), underlining a correlation between aquifer oscillation and NAPL migration. Hence, after 42 days, dual-phase samples collected at 3 m depth were dragged down with water table descent (between 27 and 42 days). In addition, groundwater samples highlighted a remarkable lateral migration of NAPL, probably due to the collapse of capillary fringe exerted by the high amount of ethanol. Twenty-five FPS were detected between 20 and 83 days after release in different wells (MW-F, MW-2, MW-5, MW-7, MW-8, MW-10, and MW-11). If they were accounted within the source region, in only 42 days, the initial spill area increased from 1.5 m^2 in the vadose zone to at least 5.6 m^2 of FPZ on the top of saturated zone. These findings suggest that high ethanol content blends can lead to the fast NAPL mobilization due to ethanol-driven cosolvency and collapse of capillary fringe, resulting in large and irregular FPZs. However, despite the complexity of FPZ dissolved ethanol/BTEX compounds in the E85 site exhibited a comparable plume evolution (Figs. 4 and 5), showing similar and uniform shapes, which is consistent with Yu et al. (2009) observations. Therefore, our data demonstrate that ethanol content or transiency of groundwater flow exerts a larger influence on dissolved plume behavior when compared to the geometry of the contamination source.

BTEX mass transfer in the E85 site was similar to an ethanol flushing of the source (Jawitz et al., 2000; Brooks et al., 2004). To exemplify, BTEX was readily transferred to the aqueous phase (the peaks occurred between 40 and 85 days) and exhibited low persistence, reaching concentrations (7 $\mu g \cdot L^{-1}$) close to remediation goals within 1600 days after release. Comparatively, such low source-zone concentrations were observed at the E24 site only after 5000 days following the release. Although the highly soluble ethanol generally dissolves earlier than BTEX (Corseuil et al., 2011a) as a result of the limited aqueous solubility of the aromatic compounds, the breakthrough curves (BTC) in E85 plot showed peak concentrations of both ethanol and BTEX at the beginning of the experiment. As compounds migrated away from the source, peak concentrations of ethanol and BTEX were concomitantly detected in the MWs located in the main groundwater flow direction, demonstrating their concurrent dissolution and migration (Fig. 8). Likewise, centroid locations also indicated a pronounced migration of ethanol and BTEX plumes in E85 site (Fig. 4, Fig. 5), which is coherent with compounds enhanced dissolution exerted by the site hydraulic effects and the high ethanol content of the gasohol blend. The decrease in ethanol and BTEX concentrations was accompanied by the production of their anaerobic metabolites acetate and methane, thus providing evidence of ethanol and BTEX biodegradation (Fig. 8c, d).

The flow field characteristics can predict the migration of dissolved contaminants plumes and thereby support the decision on the most appropriate monitoring strategy. Contaminants concentration per sampling level indicated a sinking process of the dissolved compounds in the E85. The source-zone wells revealed high contaminants concentration at the upper level (2 m bgs), whereas at distant monitoring wells (MW-23 and MW-28 – located at 10 and 14 m away from the source, respectively) contaminants concentrated on the deeper levels (5 and 6 m bgs). Likewise, as previously mentioned in Section 3.1, the same phenomenon was observed for the E24 site, although it was less pronounced. The vertical drift is directly associated with the local flow field that contributes to a downward movement of the compounds. In addition, a plume inspection along a transect located 14 m away from the source shows the highest concentrations at 4 m bgs from the western boundary (MW-27 in Fig. 9a) and 6 m bgs from the eastern boundary (MW-31 in Fig. 9c). This nonhomogeneous distribution of concentrations is probably caused by a low permeability formation

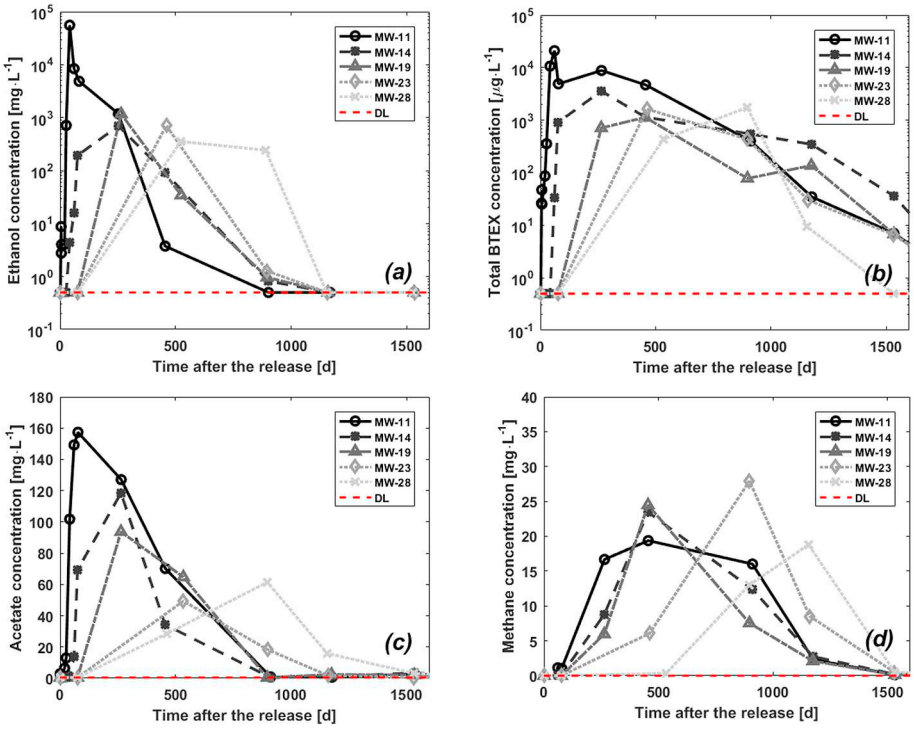

Fig. 8. Times series of BTCs along the main direction of groundwater flow: MW-11 (source zone), MW-14 (3.7 m from source), MW-19 (5.7 m from source), MW-23 (10 m from source) and MW-28 (14 m from source). Each graph represents average concentrations in the vertical profile (n = 5) of ethanol (a), total BTEX (b), acetate (c) and methane (d).

dipped towards the east that corroborates the anti-clockwise rotation of the main groundwater direction during dry periods (Supporting Information). Such changes in plume direction could be predicted with a time-series analysis of the flow field at contaminated sites. This underscores the importance of conducting a thorough hydrogeological assessment to properly select groundwater monitoring wells and track contaminants plume migration.

3.3. Ethanol and BTEX degradation kinetics

The faster dissolution of BTEX observed in the E85 site relative to E24 was attributed to the higher amount of ethanol that exerted co-solvency effect (Fig. 3). Accordingly, both BTEX and ethanol mass peaked at 85 days after the release (Fig. 11), thus demonstrating a similar dissolution dynamics. Degradation rates were determined after the onset of ethanol and BTEX biodegradation and, as they peaked concomitantly, similar initial timeframes were considered in the calculations (Table 2). Unlike E85, in the E24 site, BTEX concentrations peaked after 970 days and the onset of their biodegradation was observed only after ethanol depletion (Fig. 11). It is worth noting that control experiments with gasoline alone would be useful to quantitatively discern the effects of ethanol.

The conservative tracer (bromide) zero-order mass decrease was used to represent migration of dissolved compounds forced by groundwater flow field at both experimental sites and to estimate transport rates. Results revealed a transport rate three times higher in E85 (0.242 y^{-1}) than E24 (0.092 y^{-1}) (Table 3), which coincided with the flow field analysis (Section 3.1). This difference in mass decrease transport-related follows the ratio of seepage velocities between the sites, which can potentially avoid confounding effects in the estimation of contaminants biodegradation rates, since the area with faster flow (E85) also presented higher fitted decay rates. It worth stressing that fitted mass degradation values for ethanol and BTEX (Table 2) agreed with results reported by other studies that used different methodologies (Corseuil et al., 2011a; Corseuil et al., 2015; Ramos et al., 2016; Steiner et al., 2018). After subtracting specific transport rates from the reactive compounds degradation, the resulting first-order biodegradation rates were: ethanol 1.104 y^{-1} (E85) and 1.076 y^{-1} (E24), benzene 0.836 y^{-1}

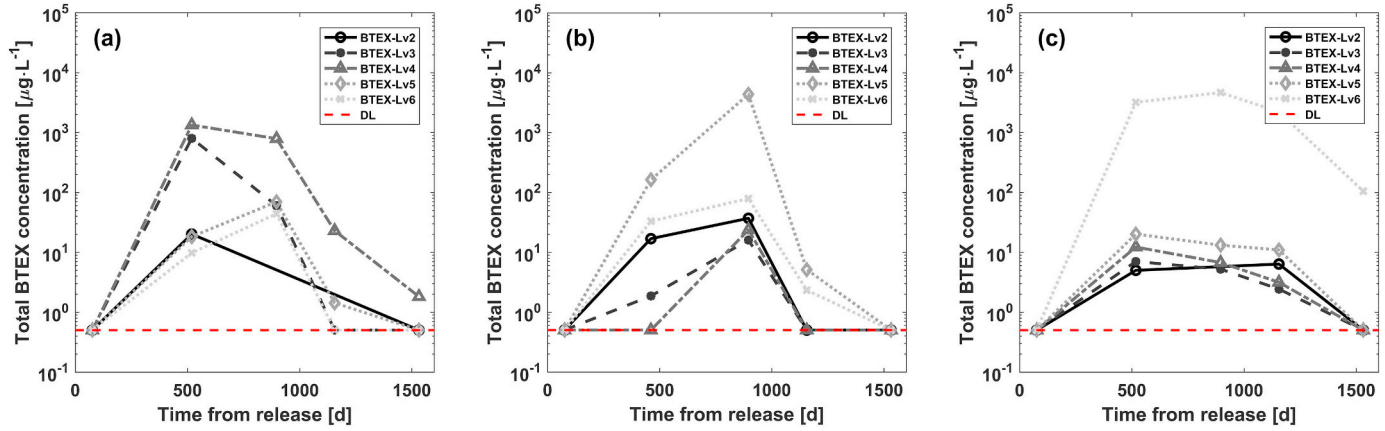

Fig. 9. Time series of BTEX BTC along transversal transect (14 m to source) from western to eastern boundary: MW-27 (a), MW-29 (b), MW-31 (c) organized per sampling depth to ground (Lv = level in meters bgs).

Table 2
Estimation of ethanol, benzene and total BTEX first-order degradation rates, and degradation rates with subtracted transport rates and quality summary for E85 and E24 sites.

Compound (Site)	Timeframe [y^{-1}]	First-order degradation rates (95% Conf. Bounds) [y^{-1}]	Degradation rates with subtracted transport rates [y^{-1}]	R^2	n
Ethanol (E85)	0.1–4.2	1.346 (0.551–2.141)	1.104	0.959	7
Ethanol (E24)	1.4–4.1	1.168 (0.590–1.756)	1.076	0.969	5
Benzene (E85)	0.2–5.2	1.078 (0.891–1.266)	0.836	0.997	7
Benzene (E24)	2.7–10.5	0.766 (0.643–0.890)	0.674	0.995	10
BTEX (E85)	0.2–5.2	1.058 (0.553–1.582)	0.816	0.981	7
BTEX (E24)	2.7–10.5	0.493 (0.403–0.584)	0.401	0.967	10

Table 3
Estimation of decay rate of bromide mass and main parameters summary for E85 and E24 sites.

Tracer (Site)	Timeframe [y^{-1}]	Zero-Order fitting rate (95% Conf. Bounds) [$g{\cdot}y^{-1}$]	Initial released mass [g]	Transport rate [y^{-1}]	R^2	n
Bromide (E85)	2.5–5.2	406.6 (203.9–609.6)	1678	0.242	0.974	4
Bromide (E24)	2.7–10.5	61.6 (53.4–69.7)	670	0.092	0.974	10

(E85) and 0.674 y^{-1} (E24) and in average for total BTEX 0.816 y^{-1} (E85) and 0.401 y^{-1} (E24) (Table 2). These values are consistent with the range of rates reported elsewhere for ethanol and BTEX compounds (Alvarez et al., 1991; Corseuil et al., 1998). Therefore, the enhanced dissolution of BTEX in E85 site led to higher biodegradation rates relative to BTEX in E24 site.

The higher BTEX biodegradation rates in E85 (relative to E24 site) could be attributed to the metabolic flux dilution phenomenon, as it predicts that removal rates are proportional to the fraction of the available substrates in the mixture (Lovanh and Alvarez, 2004). Accordingly, the metabolic flux dilution in E85 was evaluated at the source zone (MW-11) and compared with source zone (SW4) at E24 site (Corseuil et al., 2015). The enhanced dissolution (and availability) of BTEX in E85 site increased their source zone fraction in the mixture (ethanol/BTEX), as opposed to the lower dissolved BTEX concentrations and corresponding fraction in the mixture in E24 site (Fig. 10). Therefore, higher biodegradation rates were observed for BTEX in E85 site, which was likely due to their enhanced fraction in the mixture relative to E24 site. This is consistent with metabolic flux dilution that considers the simultaneous degradation of multiple substrates with compound-specific degradation rates being proportional to their relative abundance in the mixture.

The higher removal rates observed for the E85 site are coherent with the stimulation of biomass and specific hydrocarbon degraders. Accordingly, after 72 days following the release total biomass growth increased up to 2 orders of magnitude ($\approx 2.5 \times 10^9$ gene copies g^{-1}) relative to the background concentration at the source-zone ($\approx 3 \times 10^7$ gene copies g^{-1}). This is consistent with the organic compounds infiltration and dissolution into the groundwater, as they were likely used as substrates for microbial growth. The migration of dissolved contaminants away from the source (Figs. 12 and 13) was reflected by the decrease in total biomass source-zone concentration at 918 days after the release, reaching a condition similar to the background (2.9×10^7 gene copies g^{-1}) that was observed until the end of the monitoring period (4.5×10^7 gene copies g^{-1} at 1532 days after E85 release) (Fig. 12). Thus, although contaminants were partly consumed as substrates, the transport was likely the driving force as evidenced by the plume migration over the site, which justifies the return towards the original (unpolluted state) baseline microbial condition at the source zone.

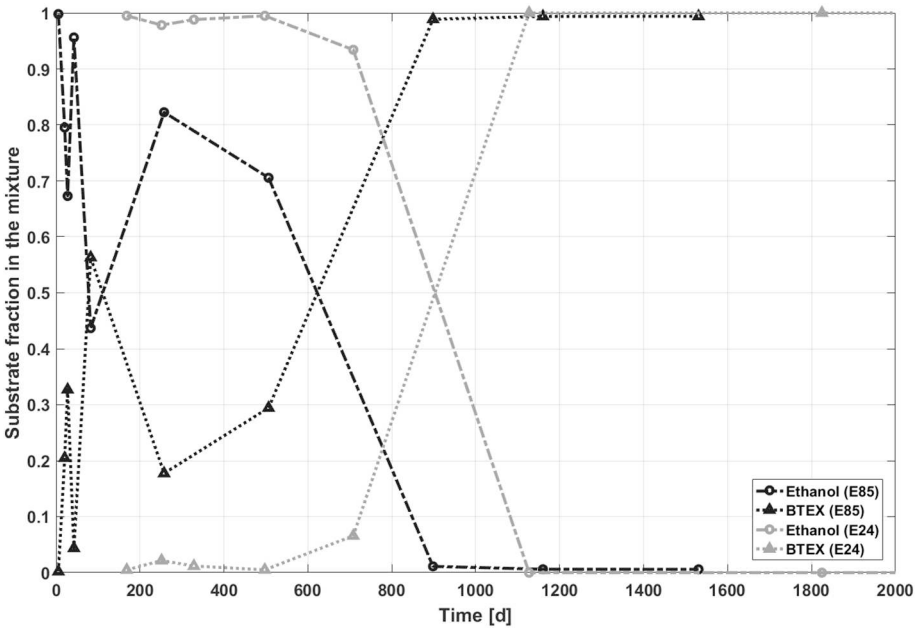

Fig. 10. Ethanol (circles) and BTEX (triangle) as total organic carbon (TOC) fractions in the mixture for E85 (MW11 – source zone) and E24 (SW4 – source zone) experiments.

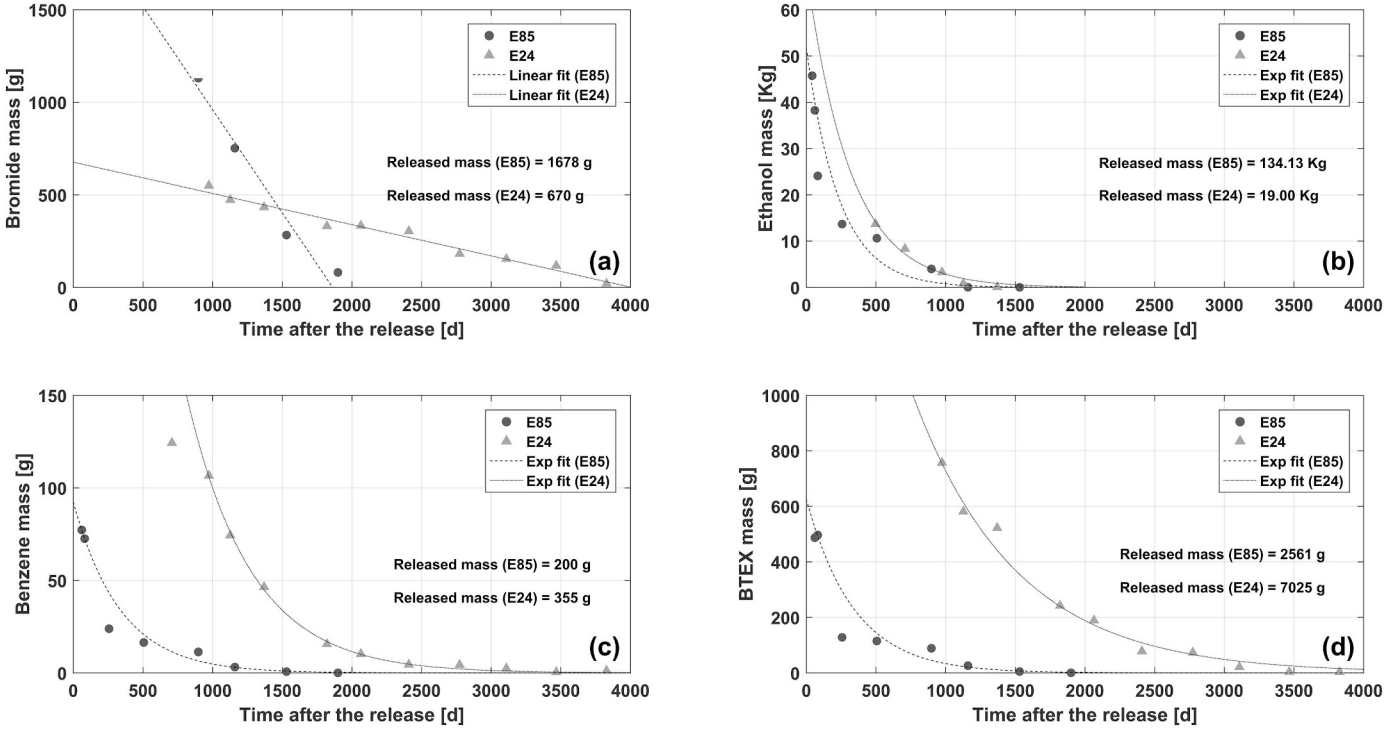

Fig. 11. Total mass decay obtained from plume interpolation for E24 and E85 sites: (a) linear fitting for bromide mass evolution, (b) exponential fitting for ethanol, (c) dissolved benzene and (d) total BTEX.

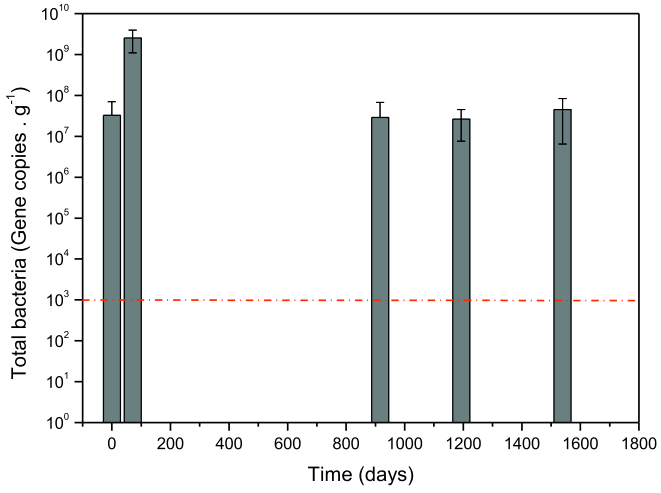

Fig. 12. Concentration of total bacteria (gene copies g^{-1}) at the source-zone of E85 experiment. Detection limit (dashed red lines) for total bacteria analysis was 10^3 gene copies g^{-1}. (For interpretation of the references to colour in this figure legend, the reader is referred to the web version of this article.)

Likewise, sequencing results revealed the presence of aromatic hydrocarbons degraders (*Gouta 19, Treponema,* WCHB1-05*, Kaistobacter, Geobacter, Rhodoplanes, Sphingomonas*)) at the monitoring wells evaluated (MW-S, MW-23 and MW-25) (Fig. 13A and B), which is coherent with their exposure to BTEX compounds. Anaerobic genera dominated wells MW-23 and MW-25, which was likely due to the presence of residual concentrations of BTEX (132 and 241 $\mu g \cdot L^{-1}$) that generally depletes the available dissolved oxygen and leads to the establishment of anaerobic zones, as evidenced by the negative ORP values (−36 and − 1 mV) and methane production (8.5 and 4 $mg \cdot L^{-1}$). Comparatively, the source-zone microbial profile at 1532 days was mainly composed by aerobic genera which can be supported by the absence of BTEX compounds at the source after 1532 days, the positive ORP value (+222 mV) and methane concentration below the detection limit (< 10 $\mu g \cdot L^{-1}$). Detailed information about the metabolism and respiration mode of the microbial genera detected in E85 site is available in the Supporting Information (Table S4). These findings provide converging lines of evidence of BTEX migration over the site and biodegradation thus, indicating that molecular biology can be used as a complementary tool for groundwater pollution monitoring, as communities shift according to the transient flow and geochemical conditions encountered at the site.

4. Conclusions

Spills of gasohol blends into phreatic aquifers subject to high recharge rates and sharp water-table fluctuations can undergo enhanced migration and degradation. Transient variations in groundwater flow velocity and direction, caused by the changes in recharge as well as geological heterogeneity, can enhance source dissolution, resulting in greater plume spreading and migration. This has significant implications for effective monitoring of groundwater pollutants and plume dynamics and lifespan. In controlled gasohol spills at Ressacada, Brazil, the sharp water-table fluctuations observed in E85 site dragged the compounds downwards, showing a fast vertical migration, while this effect was less pronounced in E24 site due to the lower hydraulic conductivity and the position of low-conductivity layers. Specific migration of bromide plumes showed significant differences in transport rates between the E85 (faster) and E24 (slower) sites, despite the fact that both sites are located at neighboring areas (400 m of distance). The higher seepage velocity in E85 relative to E24 resulted in a faster horizontal migration of plume center of mass (15 and 5 m, for E85 and E24, respectively), which underscores the critical influence of local flow field in contaminated sites assessment and the importance of subtracting flow-driven rates from the decay rates obtained by fitting field data to isolate biodegradation rates.

The high amount of ethanol in E85 site exerted cosolvency effect on BTEX and thereby enhanced their dissolution (within 85 days) and average concentrations (up to 20 $mg L^{-1}$) in groundwater. The high

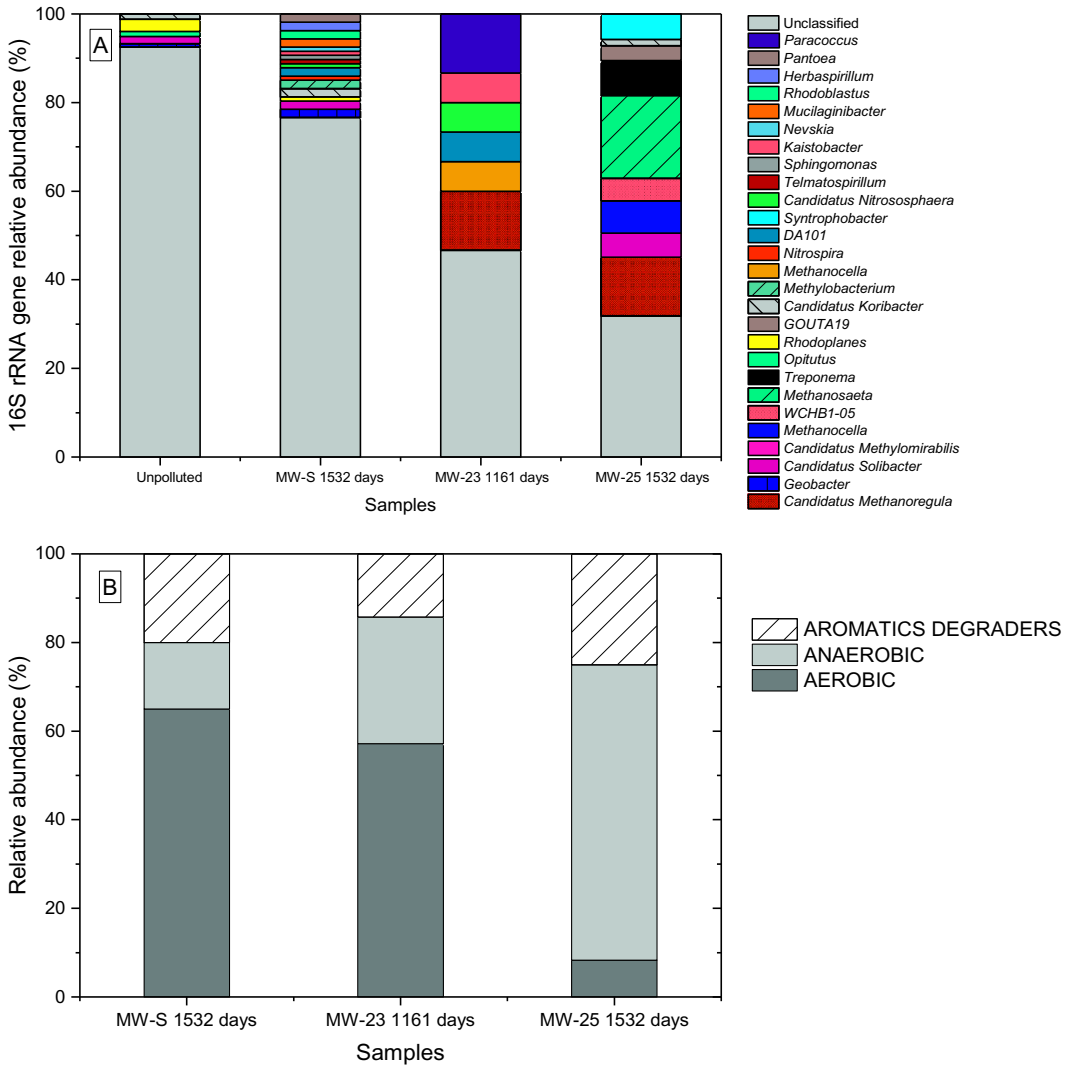

Fig. 13. (A) 16S rRNA gene relative abundance (%) of microbial communities at E85 experiment at background (unpolluted) well, MW-S (source-zone), MW-23 and MW-25. Charts depict microbial genera with a relative abundance of $^{>}$ 0.7%. (B) Microbial community respiration mode and aromatic hydrocarbons degraders relative abundance (%) in MW-S at 1532 days, MW23 at 1161 days and MW25 at 1532 days (without depicting unclassified genera). (For interpretation of the references to colour in this figure legend, the reader is referred to the web version of this article.)

concentrations of BTEX led to faster degradation rates relative to E24 site and BTEX and ethanol were biodegraded concomitantly as opposed to the often observed ethanol preferential biodegradation. This was likely attributed to the metabolic flux dilution phenomenon as the relative biodegradability of a compound in a mixture of alternative substrates is often concentration-dependent and the degradation rates are proportional to their fraction in the substrates mixture. Therefore, BTEX and ethanol were biodegraded at similar rates. Comparatively, in E24 site BTEX dissolution was significantly slower (maximum after 1000 days) and the onset of BTEX dissolution and biodegradation was only observed after ethanol depletion. Accordingly, BTEX degradation rates were slower (0.401 y^{-1} relative to 0.816 y^{-1}) and mass depletion was delayed (after 3800 days relative to 1600 days following the release) relative to E85 site. Total biomass was stimulated as ethanol and BTEX dissolved into the groundwater and shifts in microbial communities were driven by the transient flow and geochemical groundwater conditions at the E85 site. Thus, although the high amount of ethanol (in E85 site) enhanced BTEX dissolution, it led to fast degradation rates that speeded up BTEX compounds biodegradation, while their migration was determined by the local groundwater flow.

Overall, the practical implication of this work is that the groundwater flow field and high ethanol content in gasohol blends can significantly affect plume dynamics and lifespan, especially at sites under high recharge rates or fast groundwater flow. Accordingly, E85 site, due to a faster groundwater flow, showed an increased migration of contaminants relative to E24 (2.6 times higher), but also exhibited higher biodegradation rates (2.0 times higher), whilst E24 demonstrated a lower plume mobility and longer-lasting contamination due to the reduced biodegradation rates relative to E85. These factors must be carefully accounted to estimate the risk for downgradient receptors and to support decisions on monitoring plans and remedial actions. Simplified approaches that focus solely on a single component of the balance (e.g. degradation kinetics) cannot thoroughly assess plume behavior, especially in highly fluctuant or heterogeneous aquifers.

Acknowledgements

The authors want to acknowledge Fundação de Ensino e Engenharia de Santa Catarina (FEESC) and Petróleo Brasileiro (Petrobras) for the financial and material support (Project contract number: 0050.0096599.15.9). We also thank the technical staff from the Ressacada Experimental Farm and the REMA group for the field monitoring of water quality, and the PhD candidate Martina Pacifici (USP, PPGEC) for her help with the figure design. Finally, we thank Professor

Dr. Timothy Vogel (Université de Lyon) for the Illumina Miseq sequencing.

Appendix A. Supplementary data

Supplementary data to this article can be found online at https://doi.org/10.1016/j.jconhyd.2019.01.003.

References

Alvarez, P.J.J., Illman, W.A., 2006. Bioremediation and Natural Attenuation: Process Fundamentals and Mathematical Models. John Wiley & Sons, Inc, pp. 604. https://doi.org/10.1017/CBO9781107415324.004.

Alvarez, P.J.J., Anid, P.J., Vogel, T.M., 1991. Kinetics of aerobic biodegradation of benzene and toluene in sandy aquifer material. Biodegradation 2, 43–51. https://doi.org/10.1007/BF00122424.

American Public Health Association (APHA), 1992. In: Standard methods for the examination of water and wastewater. American Public Health Association, American Water Works Association and Water Pollution Control Federation, Washington DC.

Bellin, A., Dagan, G., Rubin, Y., 1996. The impact of head gradient transients on transport in heterogeneous formations: Application to the Borden Site. Water Resour. Res. 32, 2705–2713. https://doi.org/10.1029/96WR01629.

Brooks, M.C., Annable, M.D., Rao, P.S.C., Hatfield, K., Jawitz, J.W., Wise, W.R., Wood, A.L., Enfield, C.G., 2004. Controlled release, blind test of DNAPL remediation by ethanol flushing. J. Contam. Hydrol. 69, 281–297. https://doi.org/10.1016/S0169-7722(03)00158-X.

Butler Jr., J.J., 1997. The Design, Performance, and Analysis of Slug Tests (1st Edition). CRC Press, pp. 262 (9781566702300).

Cápiro, N.L., Da Silva, M.L.B., Stafford, B.P., Rixey, W.G., Alvarez, P.J.J., 2008. Microbial community response to a release of neat ethanol onto residual hydrocarbons in a pilot-scale aquifer tank. Environ. Microbiol. 10, 2236–2244. https://doi.org/10.1111/j.1462-2920.2008.01645.x.

Chapman, S.W., Parker, B.L., 2005. Plume persistence due to aquitard back diffusion following dense nonaqueous phase liquid source removal or isolation. Water Resour. Res. 41, 1–16. https://doi.org/10.1029/2005WR004224.

Cirpka, O.A., 2002. Choice of dispersion coefficients in reactive transport calculations on smoothed fields. J. Contam. Hydrol. 58, 261–282. https://doi.org/10.1016/S0169-7722(02)00039-6.

Cirpka, O.A., Frind, E.O., Helmig, R., 1999. Numerical simulation of biodegradation controlled by transverse mixing. J. Contam. Hydrol. 40, 159–182. https://doi.org/10.1016/S0169-7722(99)00044-3.

Corseuil, H.X., Fernandes, M., 1999. Efeito do etanol no aumento da solubilidade de compostos aromáticos presentes na gasolina brasileira. Rev. Eng. Sanitária e Ambient. 4, 71–75.

Corseuil, H.X., Hunt, C.S., dos Santos, R.C.F., Alvarez, P.J.J., 1998. The influence of the gasoline oxygenate ethanol on aerobic and anaerobic btx biodegradation. Water Res. 32, 2065–2072.

Corseuil, H.X., Kaipper, B.I.A., Fernandes, M., 2004. Cosolvency effect in subsurface systems contaminated with petroleum hydrocarbons and ethanol. Water Res. 38, 1449–1456. https://doi.org/10.1016/j.watres.2003.12.015.

Corseuil, H.X., Monier, A.L., Fernandes, M., Schneider, M.R., Nunes, C.C., Do Rosario, M., Alvarez, P.J.J., 2011a. BTEX plume dynamics following an ethanol blend release: Geochemical footprint and thermodynamic constraints on natural attenuation. Environ. Sci. Technol. 45, 3422–3429. https://doi.org/10.1021/es104055q.

Corseuil, H.X., Monier, A.L., Fernandes, M., Schneider, M.R., Nunes, C.C., 2011b. BTEX plume dynamics following an ethanol blend release: Geochemical footprint and thermodynamic constraints on natural attenuation - supporting Information. Environ. Sci. Technol. 23. https://doi.org/10.1117/1111.2794018.2.

Corseuil, H.X., Gomez, D.E., Schambeck, C.M., Ramos, D.T., Alvarez, P.J.J., 2015. Nitrate addition to groundwater impacted by ethanol-blended fuel accelerates ethanol removal and mitigates the associated metabolic flux dilution and inhibition of BTEX biodegradation. J. Contam. Hydrol. 174C, 1–9. https://doi.org/10.1016/j.jconhyd.2014.12.004.

Da Silva, M.L.B., Alvarez, P.J.J., 2002. Effects of Ethanol versus MTBE on Benzene, Toluene, Ethyl-benzene, and Xylene Natural Attenuation in Aquifer Columns. J. Environ. Eng. 128, 862–867. https://doi.org/10.1061/(ASCE)0733-9372(2002)128:9(862).

Davis, G.B., Barber, C., Power, T.R., Thierrin, J., Patterson, B.M., Rayner, J.L., Wu, Q., 1999. The variability and intrinsic remediation of a BTEX plume in anaerobic sulphate-rich groundwater. J. Contam. Hydrol. 36, 265–290. https://doi.org/10.1016/S0169-7722(98)00148-X.

Dentz, M., Kinzelbach, H., Attinger, S., Kinzelbach, W., 2000. Temporal behavior of a solute cloud in a heterogeneous porous medium 2. Spatially extended injection. Water Resour. Res. 36, 3605–3614.

Dobson, R., Schroth, M.H., Zeyer, J., 2007. Effect of water-table fluctuation on dissolution and biodegradation of a multi-component, light nonaqueous-phase liquid. J. Contam. Hydrol. 94, 235–248. https://doi.org/10.1016/j.jconhyd.2007.07.007.

Falta, R.W., 1998. Using phase diagrams to predict the performance of cosolvent floods for NAPL remediation. Gr. Water Monit. Remediat. Summer 94–102.

Fernandes, M., 2002. Atenuação natural de aquífero contaminado por derramamento de gasolina. PhD thesis. UFSC. Universidade Federal de Santa Catarina. Florianópolis, Brazil, pp. 233.

Fetter, C.W., 2001. Applied Hydrogeology, 4th edition. Prentice Hall, Upper Saddle River, NJ, USA, pp. 624 ISBN13 9780130882394.

Freitas, J.G., Mocanu, M.T., Zoby, J.L.G., Molson, J.W., Barker, J.F., 2011. Migration and fate of ethanol-enhanced gasoline in groundwater: a modelling analysis of a field experiment. J. Contam. Hydrol. 119, 25–43. https://doi.org/10.1016/j.jconhyd.2010.08.007.

Freyberg, D.L., 1986. A natural gradient experiment on solute transport in a sand aquifer: 2. spatial moments and the advection and dispersion of nonreactive tracers. Water Resour. Res. 22, 2031–2046.

Gineval, M.E., Splitstone, D.E., 2003. Statistical Tools for Environmental Quality Measurement. Chapter 5: Tools for Dealing with Censored Data. Chapman & Hall CRC, pp. 256 (ISBN 1-58488-157-7).

Gomez, D.E., Alvarez, P.J.J., 2010. Comparing the effects of various fuel alcohols on the natural attenuation of Benzene Plumes using a general substrate interaction model. J. Contam. Hydrol. 113, 66–76. https://doi.org/10.1016/j.jconhyd.2010.02.002.

Gomez, D.E., De Blanc, P.C., Rixey, W.G., Bedient, P.B., Alvarez, P.J.J., 2008. Modeling benzene plume elongation mechanisms exerted by ethanol using RT3D with a general substrate interaction module. Water Resour. Res. 44, 1–12. https://doi.org/10.1029/2007WR006184.

Hayashi, M., van der Kamp, G., Rosenberry, D.O., 2016. Hydrology of Prairie Wetlands: Understanding the Integrated Surface-Water and Groundwater Processes. Wetlands 36, 237–254. https://doi.org/10.1007/s13157-016-0797-9.

Henry, E.J., Smith, J.E., 2002. The effect of surface-active solutes on water flow and contaminant transport in variably saturated porous media with capillary fringe effects. J. Contam. Hydrol. 56, 247–270. https://doi.org/10.1016/S0169-7722(01)00206-6.

Jarvis, N.J., 2007. A review of non-equilibrium water flow and solute transport in soil macropores: Principles, controlling factors and consequences for water quality. Eur. J. Soil Sci. 58, 523–546. https://doi.org/10.1111/j.1365-2389.2007.00915.x.

Jawitz, J.W., Sillan, R.K., Annable, M.D., Rao, P.S.C., Warner, K., 2000. In-situ alcohol flushing of a DNAPL source zone at a dry cleaner site. Environ. Sci. Technol. 34, 3722–3729. https://doi.org/10.1021/es9913737.

Lage, I. de C., 2005. Avaliação de metodologias para determinação da permeabilidade em meios porosos: Fazenda Ressacada. MSc Thesis. UFRJ, Universidade Federal de Rio de Janeiro, Brazil, pp. 119.

Lovanh, N., Alvarez, P.J.J., 2004. Effect of ethanol, acetate, and phenol on toluene degradation activity and tod-lux expression in Pseudomonas putida TOD102: evaluation of the metabolic flux dilution model. Biotechnol. Bioeng. 86 (7), 801–808. https://doi.org/10.1002/bit.20090.

Mackay, D.M., de Sieyes, N.R., Einarson, M.D., Feris, K.P., Pappas, A.A., Wood, I.A., Jacobson, L., Justice, L.G., Noske, M.N., Scow, K.M., Wilson, J.T., 2006. Impact of Ethanol on the Natural Attenuation of Benzene, Toluene, and o -Xylene in a normally Sulfate-reducing Aquifer. Environ. Sci. Technol. 40, 6123–6130. https://doi.org/10.1021/es060505a.

McDowell, C.J., Powers, S.E., 2003. Mechanisms affecting the infiltration and distribution of ethanol-blended gasoline in the vadose zone. Environ. Sci. Technol. 37, 1803–1810. https://doi.org/10.1021/es025976l.

McDowell, C.J., Buscheck, T., Powers, S.E., 2003. Behavior of gasoline pools following a denatured ethanol spill. Ground Water 41, 746–757.

Mitchell, J.K., 1976. Fundamentals of Soil Behavior. John Wiley & Sons, Inc, New York (422p).

Molson, J.W., Barker, J.F., Frind, E.O., Schirmer, M., 2002. Modeling the impact of ethanol on the persistence of benzene in gasoline-contaminated groundwater. Water Resour. Res. 38, 4–1-4–12. https://doi.org/10.1029/2001WR000589.

Müller, J.B., Ramos, D.T., Larose, C., Fernandes, M., Lazzarin, H.S.C., Vogel, T.M., Corseuil, H.X., 2017. Combined iron and sulfate reduction biostimulation as a novel approach to enhance BTEX and PAH source-zone biodegradation in biodiesel blend-contaminated groundwater. J. Hazard. Mater. 326, 229–236. https://doi.org/10.1016/j.jhazmat.2016.12.005.

Powers, S.E., Hunt, C.S., Heermann, S.E., Corseuil, H.X., Rice, D., Corseuil, X., Rice, D., Alvarez, P.J.J., 2001. The Transport and Fate of Ethanol and BTEX in Groundwater Contaminated by Gasohol. Crit. Rev. Environ. Sci. Technol. 31, 79–123. https://doi.org/10.1080/20016491089181.

Prommer, H., Barry, D.A., Davis, G.B., 2002. Modelling of physical and reactive processes during biodegradation of a hydrocarbon plume under transient groundwater flow conditions. J. Contam. Hydrol. 59, 113–131. https://doi.org/10.1016/S0169-7722(02)00078-5.

Rama, F., Franco, D., Corseuil, H.X., 2017. Spatial and Temporal Analysis of Natural Drainage in the Ressacada Aquifer (Florianopolis, Brazil). Int. J. Environ. Sci. Dev. 8, 653–660. https://doi.org/10.18178/ijesd.2017.8.9.1033.

Rama, F., Miotlinski, K., Franco, D., Corseuil, H.X., 2018. Recharge estimation from discrete water-table datasets in a coastal shallow aquifer in a humid subtropical climate. Hydrogeol. J. 26, 1887–1902. https://doi.org/10.1007/s10040-018-1742-1.

Ramos, D.T., da Silva, M.L.B., Chiaranda, H.S., Alvarez, P.J.J., Corseuil, H.X., 2013. Biostimulation of anaerobic BTEX biodegradation under fermentative methanogenic conditions at source-zone groundwater contaminated with a biodiesel blend (B20). Biodegradation 24, 333–341. https://doi.org/10.1007/s10532-012-9589-y.

Ramos, D.T., Lazzarin, H.S.C., Alvarez, P.J.J., Vogel, T.M., Fernandes, M., do Rosário, M., Corseuil, H.X., 2016. Biodiesel presence in the source zone hinders aromatic hydrocarbons attenuation in a B20-contaminated groundwater. J. Contam. Hydrol. 193, 48–53. https://doi.org/10.1016/j.jconhyd.2016.09.002.

Rasa, E., Bekins, B.A., Mackay, D.M., de Sieyes, N.R., Wilson, J.T., Feris, K.P., Wood, I.A., Scow, K.M., 2013. Impacts of an ethanol-blended fuel release on groundwater and fate of produced methane: simulation of field observations. Water Resour. Res. 49, 4907–4926. https://doi.org/10.1002/wrcr.20382.

Rein, A., Bauer, S., Dietrich, P., Beyer, C., 2009. Influence of temporally variable groundwater flow conditions on point measurements and contaminant mass flux

estimations. J. Contam. Hydrol. 108, 118–133. https://doi.org/10.1016/j.jconhyd.2009.06.005.
Ricker, J.A., 2008. A practical method to evaluate ground water contaminant plume stability. Gr. Water Monit. Remediat. 28, 85–94. https://doi.org/10.1111/j.1745-6592.2008.00215.x.
Rolle, M., Eberhardt, C., Chiogna, G., Cirpka, O.A., Grathwohl, P., 2009. Enhancement of dilution and transverse reactive mixing in porous media: experiments and model-based interpretation. J. Contam. Hydrol. 110, 130–142. https://doi.org/10.1016/j.jconhyd.2009.10.003.
Schirmer, M., Butler, B.J., 2004. Transport behaviour and natural attenuation of organic contaminants at spill sites. Toxicology 205, 173–179. https://doi.org/10.1016/j.tox.2004.06.049.
Schirmer, M., Durrant, G.C., Molson, J.W., Frind, E.O., 2000. Influence of transient flow on contaminant biodegradation. Ground Water 39, 276–282.
Steiner, L.V., Ramos, D.T., Liedke, A.M.R., Serbent, M.P., Corseuil, H.X., 2018. Ethanol content in different gasohol blend spills influences the decision-making on remediation technologies. J. Environ. Manag. 212, 8–16. https://doi.org/10.1016/j.jenvman.2018.01.071.
Tromp-Van Meerveld, H.J., McDonnell, J.J., 2006. Threshold relations in subsurface storm-flow: 2.The fill and spill hypothesis. Water Resour. Res. 42, 1–11. https://doi.org/10.1029/2004WR003800.
Werth, C.J., Cirpka, O.A., Grathwohl, P., 2006. Enhanced mixing and reaction through flow focusing in heterogeneous porous media. Water Resour. Res. 42, 1–10. https://doi.org/10.1029/2005WR004511.
Yang, M., Annable, M.D., Jawitz, J.W., 2014. Back Diffusion from Thin Low Permeability zones. Environ. Sci. Technol. 49, 415–422.
Yu, S., Freitas, J.G., Unger, A.J.A., Barker, J.F., Chatzis, J., 2009. Simulating the evolution of an ethanol and gasoline source zone within the capillary fringe. J. Contam. Hydrol. 105, 1–17. https://doi.org/10.1016/j.jconhyd.2008.11.006.
Zhang, P., Devries, S.L., Dathe, A., Bagtzoglou, A.C., 2009. Enhanced mixing and plume containment in porous media under time-dependent oscillatory flow. Environ. Sci. Technol. 43, 6283–6288. https://doi.org/10.1021/es900854r.